HHS Public Access

Author manuscript

Curr Biol. Author manuscript; available in PMC 2019 March 19.

Published in final edited form as:

Curr Biol. 2018 March 19; 28(6): 902–914.e5. doi:10.1016/j.cub.2018.02.029.

A single-neuron chemosensory switch determines the valence of a sexually dimorphic sensory behavior

Kelli A. Fagan[1], **Jintao Luo**[2,3], **Ross C. Lagoy**[4], **Frank C. Schroeder**[5], **Dirk R. Albrecht**[4], and **Douglas S. Portman**[2,3,6,7]

[1]Neuroscience Graduate Program, University of Rochester, 601 Elmwood Ave., Rochester, NY 14610 USA

[2]DelMonte Institute for Neuroscience, University of Rochester, 601 Elmwood Ave., Rochester, NY 14610 USA

[3]Center for Neurotherapeutics Development, University of Rochester, 601 Elmwood Ave., Rochester, NY 14610 USA

[4]Department of Biomedical Engineering, Worcester Polytechnic Institute, 60 Prescott Street, Room 4004, Worcester, MA 01605 USA

[5]Boyce Thompson Institute, 533 Tower Road, Ithaca, NY 14853, USA

[6]Departments of Biomedical Genetics, Neuroscience, and Biology, University of Rochester, 601 Elmwood Ave., Box 645, Rochester, NY 14610 USA

SUMMARY

Biological sex, a fundamental dimension of internal state, can modulate neural circuits to generate behavioral variation. Understanding how and why circuits are tuned by sex can provide important insights into neural and behavioral plasticity. Here, we find that sexually dimorphic behavioral responses to *C. elegans* ascaroside sex pheromones are implemented by the functional modulation of shared chemosensory circuitry. In particular, the sexual state of a single sensory neuron pair, ADF, determines the nature of an animal's behavioral response regardless of the sex of the rest of the body. Genetic feminization of ADF causes males to be repelled by, rather than attracted to, ascarosides, while masculinization of ADF has the opposite effect in hermaphrodites. When ADF is ablated, both sexes are weakly repelled by ascarosides. Genetic sex modulates ADF function by tuning chemosensation: though ADF is functional in both sexes, it detects the ascaroside ascr#3

Author contact: douglas.portman@rochester.edu.
[7]Lead contact

DECLARATION OF INTERESTS

The authors declare no competing interests.

AUTHOR CONTRIBUTIONS

Conceptualization, K.A.F., J.L., R.C.L., D.R.A., and D.S.P.; Methodology, K.A.F., R.C.L., D.R.A., and D.S.P.; Investigation, K.A.F., J.L., and R.C.L.; Resources, F.C.S.; Writing — Original Draft, K.A.F., R.C.L., and D.S.P.; Writing — Review & Editing, K.A.F., R.C.L., J.L, F.C.S., D.R.A., and D.S.P.; Supervision, D.R.A. and D.S.P.; Funding Acquisition, K.A.F., D.R.A., and D.S.P.

only in males, a consequence of cell-autonomous action of the master sexual regulator *tra-1*. This occurs in part through the conserved DM-domain gene *mab-3*, which promotes the male state of ADF. The sexual modulation of ADF has a key role in reproductive fitness, as feminization or ablation of ADF renders males unable to use ascarosides to locate mates. Our results reveal an economical mechanism in which sex-specific behavioral valence arises through the cell-autonomous regulation of a chemosensory switch by genetic sex, allowing a social cue with salience for both sexes to elicit navigational responses commensurate with the differing needs of each.

eTOC BLURB

In nematodes, some sex pheromones elicit attraction in males and repulsion in hermaphrodites. Here, Fagan et al. find the sexual state of a single pair of neurons governs this difference regardless of the sex of the rest of the body. Sex-specific sensory tuning allows a cue with salience to both sexes to evoke distinct behavioral responses in each.

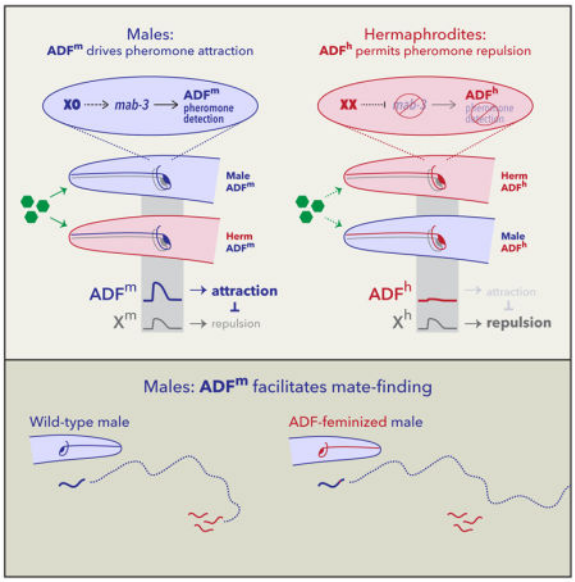

INTRODUCTION

Sex differences in behavior provide a powerful framework for identifying mechanisms that sculpt naturally occurring behavioral variation [1–4]. These differences exist along a wide spectrum, ranging from innate, sex-specific, completely divergent behavioral programs, to subtle, population-level tendencies to behave differently under specific conditions [5]. Simpler model systems afford the advantage that the effects of biological sex on neural development and function can be largely (though see [6]) dissociated from the social influences that can cause apparent sex differences in more complex animals. In both *Drosophila* and *C. elegans*, biological sex regulates multiple aspects of neuronal development, including neurogenesis and neuronal connectivity [7–13]. However, the mechanisms by which sex influences behavior, and the roles of shared neural circuits in these processes, are largely unknown.

In the nematode *C. elegans*, hermaphrodites (somatically female animals that transiently generate self-sperm) are self-fertile for much of their reproductive lifespan. Males, however, require a mate in order to reproduce, making the ability to locate hermaphrodites crucial to their fitness. Because nematode navigation relies heavily on chemosensory cues, pheromones are likely to be especially important to this process. Accordingly, multiple studies have described the ability of hermaphrodite-secreted compounds to attract males [14–18]. The most well-characterized of these attractants are members of the ascaroside family [19], several of which elicit concentration-dependent, sexually dimorphic behavioral responses alone and in combination [16, 17, 20, 21]. In particular, specific concentrations of ascr#3 (also known as C9 and asc-ΔC9) trigger attractive responses in males and, depending on neuromodulatory state, aversion in hermaphrodites [16, 20, 22, 23].

The neural and genetic underpinnings of sex differences in ascaroside-elicited behavior involve multiple mechanisms and are incompletely understood. One mechanism is anatomical: the ascr#3- and ascr#8-sensitive CEM “cephalic companion” sensory neurons are present only in males [24, 25]. Ablation of these four cells reduces ascr#3 attraction, but a substantial sex difference in behavior remains in their absence [16]. Ascaroside detection also involves shared chemosensory circuitry. In both sexes, the ASK amphid neurons detect ascr#3 and promote attraction [16, 22], though again, ASK-ablated males retain some ascr#3 attraction [16, 20]. The influence of CEM and ASK is counteracted by the ADL amphid neurons, which also detect ascr#3 but elicit an aversive response [20]. ADL responds to ascr#3 stimulation in both sexes, but the magnitude of this response is somewhat greater in hermaphrodites than males [20]. Despite these findings, the mechanisms by which shared pheromone detection circuits are functionally tuned by sex remain unknown, as does the role of such tuning in generating sexually dimorphic behavior.

Ultimately, all sex differences in *C. elegans* are controlled by chromosomal sex. Through a well-characterized genetic hierarchy, the X-to-autosome ratio determines somatic sex by regulating the autosomal transcription factor TRA-1A [26]. High TRA-1A activity specifies hermaphrodite development and function, while low or absent TRA-1A promotes male development and function. Downstream of TRA-1A, multiple targets control specific sexually differentiated features. Interestingly, several of these targets are members of the DMRT (*doublesex* and *mab-3*-related transcript) or DM-domain family, having conserved roles in the otherwise rapidly evolving mechanisms of animal sex determination [27, 28]. In *C. elegans*, members of this family regulate neurogenesis [8, 29, 30], cell fate specification [31, 32], and circuit connectivity [13, 33]. However, while biological sex also modulates the physiology of shared circuitry in *C. elegans* [15, 20, 34–37], whether DMRT genes contribute to this process is unknown.

Because TRA-1A acts cell-autonomously, cell-type-specific manipulation of its activity generates sexually mosaic animals, allowing sexually dimorphic phenotypes to be mapped to specific anatomical foci [38]. Here, we use this as an entry point to probe the underpinnings of sexual dimorphism in ascaroside responses, identifying a chemosensory switch that determines the valence of pheromone response by modulating the properties of a single pair of shared sensory neurons.

RESULTS

An ascaroside mixture elicits male-specific, CEM-independent attraction

To measure behavioral responses to ascarosides, we used an ascaroside mixture (ascr#2:ascr#3:ascr#8, 1 μM:1 μM:10 μM) shown previously to potently attract males [16, 17]. We spotted 1 μL drops of this or control solution onto opposing quadrants of a thin bacterial lawn, and ten young adult animals were placed in the center (Figure 1A). As expected, males preferentially occupied the ascaroside-containing quadrants over the subsequent 90 minutes, while hermaphrodites were modestly repelled from these regions (Figure 1B, S1A). Though weak, this hermaphrodite response reflects genuine repulsion, as it is significantly different from the behavior of animals on quadrant plates lacking ascaroside stimuli (Figure S1B). To determine whether male attraction is a direct response to ascarosides, or if it instead reflects an indirect effect of ascarosides on worm–worm interactions, we tested solitary males in the quadrant assay. These animals behaved similarly to those tested in groups of ten (Figure S1C). Furthermore, we found no evidence that this ascaroside mixture promoted male clumping or aggregation (Figure S1D). Thus, this assay reveals a clear sex difference in the valence of the behavioral response to ascarosides.

To evaluate the role of the male-specific CEM sensory neurons, we used *ceh-30(lf)* mutants, in which these neurons fail to develop [39, 40]. Unexpectedly, this revealed no detectable impairment in ascaroside attraction (Figure 1C), suggesting that the roles of different pheromone-detecting neurons depend on behavioral context. Furthermore, *ceh- 30(gf)* hermaphrodites, which possess CEM neurons, did not display pheromone attraction (Figure S1E). Since the CEMs are the only sex-specific sensory neurons in the *C. elegans* head, this result suggests that behavior in this assay might depend on sex-specific modulation of shared circuits.

Sexual modulation of shared sensory neurons regulates pheromone attraction

To assess the potential for such modulation, we manipulated the sex-determination pathway in post-mitotic neurons. In males, pan-neuronal expression of the *tra-1* activator *tra- 2(ic)* [41] feminizes the state of the nervous system but leaves male-specific neurons, as well as the rest of the body, intact [35]. Males carrying this pan-neural feminizing transgene exhibited no pheromone attraction; rather, they showed weak repulsion, reminiscent of control hermaphrodites (Figure 1D). The reciprocal manipulation, genetic masculinization of the hermaphrodite nervous system, can be achieved by pan-neuronal expression of the *tra-1* inhibitor *fem-3* [15, 34]. This too led to a marked change in behavior: masculinized hermaphrodites were attracted to ascarosides, behaving similarly to control males (Figure 1E). Thus, sexual modulation of shared neurons has a central role in generating sex-typical ascaroside attraction.

We hypothesized that the modulation of shared sensory neurons might play a role in regulating ascaroside response. Using a subtype-specific promoter to sex-reverse all ciliated sensory neurons [42], we obtained results qualitatively similar to those above: reciprocal changes were seen in both males and hermaphrodites (Figures 1F, G). The magnitude of these effects appeared smaller than those seen in pan-neural sex-reversed strains, which

could reflect differences in transgene expression or might indicate an influence of other sex-specific features. Regardless, these findings support a key role for regulated sensory function in generating sexually dimorphic pheromone attraction.

The male state of ADF promotes ascaroside attraction

We next targeted specific sensory neuron classes for sex-reversal. Despite clear roles for the ASK and ADL neurons in behavioral responses to ascr#3 [16, 20, 22], feminization of these neurons did not have marked effects on ascaroside attraction in the quadrant assay (Figure 2A). We also feminized ASI and ASJ, as these neurons are implicated in pheromone detection in other contexts [22, 43]. Again, neither manipulation had a detectable effect on ascaroside attraction (Figures 2B, C). These results do not rule out the possibility that sexual modulation of some or all of these neurons contributes to ascaroside chemotaxis, but if such roles exist, they are likely minor. Furthermore, any non-sex-specific roles for these neurons in ascaroside attraction or repulsion would not be revealed by these experiments.

In contrast, feminization of the ADF chemosensory neurons led to a striking change in behavior: like wild-type hermaphrodites, ADF-feminized males were repelled from the ascaroside-containing quadrants (Figure 2D). Moreover, masculinization of ADF in otherwise wild-type hermaphrodites was sufficient to generate marked pheromone attraction (Figure 2E). These results indicate that male-typical characteristics of ADF are necessary for pheromone attraction and, furthermore, that ADF's sexual state specifies the valence of the behavioral response elicited by pheromones. Consistent with this interpretation, the pheromone attraction elicited in hermaphrodites by pan-neural masculinization was suppressed by blocking the masculinization of ADF (Figure S2). The ability of ADF masculinization to enable pheromone attraction in hermaphrodites strongly suggests that this behavior requires no sex differences postsynaptic to ADF; that is, ADF signaling likely engages shared navigational circuits to generate sex-specific behavior.

These observations are consistent with two alternative mechanisms. In the first, the male state of ADF would enable pheromone attraction, counteracting repulsive influence(s) present in both sexes. In the second, the hermaphrodite state of ADF would actively promote repulsion, allowing a non-sex-specific attractive drive to predominate only in males. To distinguish between these, we used a split-caspase strategy to ablate ADF [44, 45]. In males, this eliminated attraction and revealed an underlying repulsive drive, but in hermaphrodites, it had minimal effects (Figure 2F). Thus, the male ADF promotes ascaroside attraction, and a parallel influence appears to promote repulsion in both sexes (Figure 2G). Notably, ADF ablation eliminated the sex difference in behavior (Figure 2F), again demonstrating that its sexual state instructively determines behavioral valence.

ADF's genetic sex determines its ability to detect ascarosides

To understand how sexual state influences ADF's response to the ascaroside mixture, we measured calcium activity via GCaMP3 fluorescence in worms exposed to pheromone stimuli in a microfluidic arena [46, 47]. Stimulation of males with the ascr#2/#3/#8 mixture elicited robust activation of ADF (Figure 3A). In contrast, ADF appeared completely unresponsive to ascr#2/#3/#8 stimulation in hermaphrodites (Figure 3B), demonstrating that

genetic sex modulates ADF's sensitivity to ascaroside stimulation. Consistent with this, ADF-specific feminization significantly reduced this neuron's responsiveness to ascaroside stimulation: 10 of the 14 ADF-feminized males tested exhibited weak or undetectable calcium responses, while only four of the 22 control males tested failed to respond (Figure 3A). Furthermore, most of the ADF-masculinized hermaphrodites tested showed strong ascaroside-induced calcium transients (Figure 3B), indicating that "maleness" is sufficient to render ADF ascaroside-responsive in hermaphrodites.

To ask whether ADF might detects ascarosides directly, we imaged activity in *unc-13* mutants, in which chemical synapses are severely compromised [48]. These animals exhibited strong, sexually dimorphic responses to ascaroside stimulation in ADF (Figure 3C). While we cannot rule out the possibility that ascaroside signals are transmitted from other neurons to ADF through gap junctions, electrical connectivity to ADF is sparse and features no obvious male-specific synapses [49] (wormwiring.org). Therefore, our results indicate that genetic sex modulates the chemosensory tuning of ADF, allowing it to detect ascarosides only in males.

We also recorded ADF's response to individual ascarosides in males. Stimulation with ascr#2 or ascr#8 alone generated weak responses, but stimulation with ascr#3 alone elicited calcium transients comparable to those seen with the ascr#2/#3/#8 mixture (Figure S3). Consistent with this, male behavior in quadrant assays using ascr#3 alone (Figure 4A) was similar to that seen with the ascr#2/#3/#8 mixture (Figure 1B). Thus, modulation of ADF's ability to detect ascr#3 is likely to be the predominant contributor to sex differences in response to the ascr#2/#3/#8 mixture.

A straightforward explanation for the sexually dimorphic ability of ADF to detect ascr#3 could be the differential expression of an ascaroside chemoreceptor. Of the eight known or putative ascaroside receptors in *C. elegans* (*srbc-64* and *srbc-66* [50], *srg-36* and *srg-37* [51], *daf-37* and *daf-38* [52], and *srx-43* and *srx-44* [53, 54]), none are known to be expressed in ADF in either sex, making these unlikely candidates. Another putative chemoreceptor, *srd-1*, is expressed male-specifically in ADF [55], but we observed no pheromone attraction defects in *srd-1(eh1)* null mutants (Figure S4A). Thus, it remains unclear whether differential receptor expression underlies the sex difference in ADF physiology.

Because ADF is one of the few serotonergic neurons in *C. elegans*, we asked whether serotonin was important for ADF-mediated pheromone attraction. However, males lacking *tph- 1* (tryptophan hydroxylase, necessary for serotonin biosynthesis) exhibited wild-type pheromone attraction (Figure S4B). Thus, ADF likely uses other mechanisms to communicate pheromone detection to downstream circuits.

The DMRT gene *mab-3* links genetic sex to modulation of ADF function

To understand how ADF's sexual state modulates its ascaroside sensitivity, we considered known targets of *tra-1*. One of these, *mab-3*, is a founding member of the DMRT or DM-domain family of transcriptional regulators [56]. These genes have roles in sex determination and sexual differentiation in a wide variety of invertebrate and vertebrate species [27, 28]. In *C. elegans*, *mab-3* implements male-specific features of neurogenesis,

intestinal physiology, and tail tip morphology [8, 29, 57]; it also promotes male exploratory behavior [30]. However, a role for *mab-3* in the modulation of neural circuit function has not been noted; indeed, such a role for DMRT genes in any species is not well described.

Interestingly, the only described site of *mab-3* expression among shared neurons is ADF, where its expression is male-specific [30]. We found that *mab-3* mutant males exhibited significantly reduced attraction to ascr#3 and to the ascr#2/#3/#8 mixture, while *mab-3* hermaphrodites appeared wild-type (Figure 4A, Figure S4C). Expression of *mab-3(+)* under the control of an ADF-specific promoter rescued the reduced ascr#3 attraction of *mab-3* males (Figure 4B), strongly suggesting that this gene acts cell-autonomously to promote ADF's male-specific function. Consistent with this, loss of *mab-3* had no further effect on behavior when ADF was genetically ablated in males (Figure 4D).

To confirm that *mab-3* functions downstream of *tra-1* in ADF, we examined *MAB-3::GFP* expression. As expected, GFP was detectible in ADF in males but not in hermaphrodites; furthermore, masculinization of ADF was sufficient to activate *MAB-3::GFP* in this cell (Figure 4E). *mab-3* was also partially required for the ascr#3 attraction generated by ADF masculinization in hermaphrodites (Figure 4F). Notably, however, loss of *mab-3* did not completely eliminate ascaroside attraction in males or in ADF-masculinized hermaphrodites (Figures 4A, F). In addition, ectopic expression of *mab-3* in the hermaphrodite ADF was insufficient to generate attraction (Figure 4C). Therefore, *mab-3* likely acts together with *tra-1* target(s) to bring about the fully masculinized state of the male ADF.

The sex-specific tuning of ADF facilitates mate-searching

Our results using synthetic ascarosides suggest that sexual modulation of ADF allows males to use ascarosides as mate-location cues. However, the ascaroside concentrations that males would need to recognize for this purpose [21, 58] are likely to be significantly lower than those used in the quadrant assay, where small drops of 1 μM ascr#3 are expected to diffuse to the mid-nanomolar range. Furthermore, hermaphrodites secrete complex mixtures of ascarosides (and other compounds) whose composition varies according to multiple factors [59–61]. Indeed, whether *C. elegans* males are capable of locating mates using the ascarosides they produce has, to our knowledge, not been reported.

To explore these issues, we asked whether wild-type males could distinguish between wild-type and *daf-22* mutant hermaphrodites, which lack the ability to synthesize short-chain ascarosides including ascr#2, ascr#3, ascr#8 [16, 17, 62, 63]. In these experiments, we adapted the quadrant assay to use genetically immobilized (*unc-13*) hermaphrodites, rather than synthetic ascarosides, as stimuli (Figure 5A). We found that wild-type males robustly chose to associate with *unc-13* over *unc-13; daf-22* hermaphrodites (Figure 5B), demonstrating that males do indeed rely on hermaphrodite ascaroside production to identify potential mates. Wild-type hermaphrodites displayed no such preference, distributing themselves equally among quadrants containing *unc-13* and *unc-13; daf-22* hermaphrodites (Figure 5B). Furthermore, the ability of males to detect ascarosides in this context depended heavily on the sexual modulation of ADF: feminization of ADF significantly reduced the preference of males for associating with pheromone-producing hermaphrodites. Moreover, ADF ablation rendered males barely able to distinguish between the two populations (Figure

5B). Together, these findings establish a central role for ADF in males' ability to respond to ascaroside stimuli encountered in an ethologically relevant context. Wild-type hermaphrodites exhibited no preference for either population of immobilized hermaphrodites, and neither ADF masculinization nor ADF ablation altered their behavior (Figure 5B). Thus, "maleness" in ADF alone appears insufficient alter hermaphrodite behavior in this context, suggesting that matepreference behavior in this assay depends on more than the detection of ascr#3 by ADF (see Discussion).

To better understand the effects of hermaphrodite-produced ascarosides on male behavior, we placed single males on a small food lawn 2.5 cm away from a single *unc-13* adult hermaphrodite (Figure 5C) and monitored male position and behavior at five-minute intervals. Under these conditions, roughly 70% of control males located the hermaphrodite and initiated copulatory behavior within 60 min (Figure 5C). ADL- and ASK-feminized males behaved comparably to wild-type, but ADF-feminized males were significantly impaired in this task, with fewer than 50% initiating copulation within the same time frame (Figure 5C). This is not likely to be secondary to other causes, as we found no difference in exploratory activity between control and ADF-feminized males (Figure S5A), and ADF-feminized males exhibited no significant reduction in their propensity to initiate mating once hermaphrodite contact occurred (Figure S5B). These results suggest that the male state of ADF allows males to use hermaphrodite-derived ascarosides as navigational cues.

We next asked whether ascaroside production was necessary for the ability of ADF to promote mate-finding. In these experiments, we placed single males ~2 cm from a group of three hermaphrodites (Figure 5D) and scored male behavior using recorded video. We found that males took significantly longer to initiate copulation with *unc-13; daf-22* hermaphrodites compared to control *unc-13* hermaphrodites (Figure 5D). This is not explained by a defect in copulatory behavior itself: male contact-response efficiency was not compromised by a loss of ascaroside production by its mate (Figure S5C). The ability of ADF-feminized males to locate mates and initiate copulation, already reduced compared to WT animals, was not further degraded by pairing them with *daf-22* mutant hermaphrodites (Figure 5D). Thus, ADF facilitates the ability of males to use hermaphrodite-derived ascarosides as navigational cues. Unexpectedly, WT males appeared to locate *daf-22* hermaphrodites even less efficiently than did ADF-feminized males, though this difference was only marginally significant ($p = 0.093$) (Figure 5D). If biologically meaningful, this result might suggest that ADF feminization triggers the development of compensatory, ascaroside-independent sensory mechanisms.

DISCUSSION

Pheromone attraction provides an ideal entry point for understanding the genetic, developmental, and physiological mechanisms that bring about naturally occurring, adaptive behavioral variation [64]. Here, we find that the genetic sex of a single pair of *C. elegans* head chemosensory neurons, ADF, determines whether animals will mount male-typical (attraction) or hermaphrodite-typical (repulsion) responses to sex pheromones (Figure 6). ADF promotes pheromone attraction by detecting the ascaroside pheromone ascr#3 only in males, a result of cell-autonomous regulation by the terminal sexual regulator *tra-1* and its

direct target *mab-3*, a conserved DMRT gene [27, 28]. The detection of pheromone by ADF overrides an innate repulsion response to these pheromones present in both sexes, thereby allowing males to use ascarosides as navigational cues that facilitate mate-finding. Thus, the sex-dependent chemosensory tuning of a single pair of sensory neurons generates differential behavioral responses to a cue that has salience for both sexes, but to which opposite responses seem beneficial.

A role for ADF in sex pheromone attraction has not been previously described. Early experiments indicated that the larval ADF neurons might detect dauer pheromone [43], also an ascaroside-dependent activity. In hermaphrodites, ADF is best known for the modulation of food-dependent behaviors and the release of serotonin [43, 65–68]. The possibility that the requirement for ADF in male pheromone attraction stems only from its ability to signal food seems unlikely for several reasons. First, such a signal would be expected to be serotonin-dependent, but we find that male pheromone attraction does not require serotonin. Second, such a signal would not be expected to require the male state of ADF. Third, the response of ADF to ascaroside stimulation in *unc-13* mutants strongly suggests that it detects ascarosides directly. We cannot rule out the possibility that sex-specific connectivity contributes to the sexually dimorphic function of ADF; however, ongoing connectomics studies have revealed no male-specific chemical or electrical synapses involving ADF (wormwiring.org).

ADF does not act alone in the detection of ascaroside sex pheromones—at least three additional *C. elegans* sensory neuron types, CEM, ASK, and ADL, are also implicated in ascaroside-elicited behaviors [16, 20, 22] (Figure 6). The CEMs, the only male-specific head sensory neurons [25], respond to ascaroside stimulation with a complex pattern of activity that may facilitate the detection of changes in ascaroside concentration [24]. Why our assay reveals no effect of CEM loss is unclear, but likely reflects dependencies on the concentration and diffusion of the stimulus as well as the specific behavioral responses being measured. The ASK neurons respond to ascaroside stimulation in both sexes [22], explaining why a prominent role for sexual modulation of ASK was not revealed by our studies. The ADL neurons, unlike the CEMs and ASK, promote aversion to ascr#3 in hermaphrodites. ADL detects ascarosides in both sexes, but its response is blunted in males [20]. This makes ADL a strong candidate for mediating the underlying repulsive behavior revealed by feminizing or ablating of ADF in males, indicated by neuron “X” in Figure 2G.

How genetic sex modulates the function of shared circuits is an open question, with clear relevance for understanding typical sex differences in the brain and the mechanisms that generate sex-biased susceptibility to or protection from neurological and neuropsychiatric disorders [69, 70]. We find here that the DMRT transcription factor *mab*-3 couples chromosomal sex to the functional modulation of ADF. In *C. elegans*, genes in this family have been implicated in male-specific morphogenesis, neurogenesis, and circuit connectivity [8, 13, 29–31, 33, 57], but not the physiology of shared circuits. In Drosophila, the DMRT gene *doublesex* has important functions in neurogenesis and cell death, but circuit connectivity and behavior are largely controlled by the insect-specific transcription factor *fruitless* [71]. In neither of these systems have DMRT genes been found to directly modulate the functional characteristics of sexually isomorphic circuits. Consistent with the male-

specific expression of *mab-3* in ADF [30], we found that this gene acts cell-autonomously to promote ascaroside attraction, and that *mab-3* is required for the full effects of ADF masculinization on hermaphrodite behavior. These results reveal a new role for DMRT genes in the modulation of the physiological properties of shared neurons, further solidifying their central role in sculpting sex-specific features of the invertebrate nervous system. Because *mab-3* expression in ADF in hermaphrodites appears insufficient to generate pheromone attraction, and because *mab-3* loss in males only partially compromises pheromone attraction, it is likely that additional factor(s) act together with *mab-3*, downstream of *tra-1*, to fully masculinize ADF. Identifying these factors, as well as their downstream targets, will be an important focus of future work.

Because ADF masculinization is sufficient to sensitize this neuron to ascarosides and to generate an attractive response to them in hermaphrodites, no sex-specific features post-synaptic to ADF seem to be necessary for ascr#3 attraction. An appealing idea is that male-specific ascaroside detection results from the regulation of ascaroside chemoreceptor(s) by genetic sex; testing this model will require further studies. Regardless, our results reinforce the idea that sex differences in behavior can emerge not only via sex-specific circuits but also through the differential activation of programs common to both sexes [72–74]. Here, we favor the idea that ascaroside detection by the male ADF differentially engages shared navigational circuits. Indeed, ADF activation is associated with locomotor slowing in hermaphrodites [66, 68], suggesting that sex-specific detection of ascarosides by ADF might trigger a dwelling or local-search-like state that enables males to more thoroughly investigate their immediate surroundings. Exposure to ascr#3-containing plates has been shown to increase male reversal rate [16], further supporting this idea.

Our results also reveal that males prefer to associate with ascaroside-producing, over ascaroside-lacking, hermaphrodites, demonstrating that these compounds, even in the small amounts produced by individual hermaphrodites, can be employed as navigational cues by males. Furthermore, we find that the male state of ADF is necessary for this ability, supporting an important role for ADF in mate-finding in ecologically relevant contexts. However, ADF “maleness” is insufficient for this behavior, as ADF-masculinized hermaphrodites show no preference for associating with ascaroside-producing hermaphrodites. This could indicate that the preference of males for ascaroside-producing hermaphrodites also depends on sex-specific characteristics of other amphid chemosensory neurons; it might also suggest that pheromones produced by the ADF-masculinized hermaphrodites themselves interfere with this behavior. This apparent insufficiency of ADF sexual state could also result from a requirement for copulatory structures in the male tail, particularly the sensory rays, in maintaining contact with ascaroside-producing hermaphrodites once animals have navigated to them.

In insects, sex differences in behavioral responses to sex pheromones emerge through multiple mechanisms. Significant attention has been paid to the role of the sex-specific processing of chemosensory information, largely as a result of sexually dimorphic circuits [9, 11, 75]. Sex differences in the number and connectivity of sensory structures also have important roles [76, 77]. Interestingly, like in *C. elegans,* insect chemosensory structures can

also be sexspecifically tuned [78]. Thus, simply regulating the perception of a stimulus may be an efficient and conserved mechanism for generating sex-specific attention.

Sexual modulation of shared chemosensory circuits appears to be a key regulator of behavioral prioritization and decision making in *C. elegans*. Jang *et al.* found that ADL responses to ascr#3 differ by sex [20], and the shared chemosensory neuron ASJ produces the neuromodulatory TGFβ ligand DAF-7 only in males, thereby influencing mate-searching behavior [37]. Unidentified, non-ascaroside sex pheromones described by White *et al.* [15] also exert sex-specific effects through modulation of sensory function. In this case, the ASI sensory neurons have been suggested to repress sex pheromone attraction in hermaphrodites [79], though this seems not to apply to ascarosides. The findings we report here on ADF have interesting parallels in another sensory neuron, AWA, in which a sex difference in expression of the chemoreceptor ODR-10 alters the attraction to the food-related cue diacetyl and to bacterial food itself, allowing well-fed adult males to prioritize mate-searching over feeding [34, 36]. Notably, other aspects of internal state regulate chemosensory function in *C. elegans* [23, 36, 80–89] and other systems, including insects, rodents, and humans [90–94]. Thus, sex differences in chemosensory tuning can be considered instances of more general mechanisms that generate flexibility in sensory circuit function.

A hallmark of nervous systems is their ability to detect and respond to stimuli in a manner commensurate with internal and external conditions. Neuromodulation is central to this state-dependence, generating plasticity in behavior by reconfiguring circuit dynamics [95, 96]. With regard to some aspects of internal state—e.g., hunger, sleep, and aggression [97–99]—significant progress has been made in the role of neuromodulation. Though biological sex is also deeply conserved dimension of internal state, how it influences circuit function is poorly understood. Continued studies of the mechanisms by which biological sex regulates neuronal function, particularly in the context of sex-shared circuits, are likely to shed light on these issues.

STAR METHODS

CONTACT FOR REAGENT AND RESOURCE SHARING

Further information and requests for resources and reagents should be directed to and will be fulfilled by the Lead Contact, Douglas Portman (douglas.portman@rochester.edu).

EXPERIMENTAL MODEL AND SUBJECT DETAILS

The experimental model in these studies is the nematode *C. elegans.* Strains were obtained from the *Caenorhabditis* Genetics Center, other laboratories, or constructed in our laboratory as detailed in the Key Resources Table. Cultures were grown at 20°C using Nematode Growth Medium (NGM) seeded with *E. coli* OP50 per standard methods [100]. The two sexes of *C. elegans* are hermaphrodites and males; both sexes were used extensively in this work. Because the wild-type strain N2 generates very few male progeny under standard culture conditions, all strains used in this work contained the mutation *him-5(e1490) V*, unless otherwise noted. This mutation increases the frequency of males in self-progeny

broods to ~30–35%, and we refer in this paper to *him-5(e1490) V* as the wild-type or control strain. All behavioral assays were carried out on one-day old adult animals, obtained by picking L4 animals from mixed-sex plates onto same-sex holding plates overnight. In strains harboring extrachromosomal array transgenes, non-transgenic siblings were used as the control population.

METHOD DETAILS

Molecular Biology and Construction of Transgenic Strains—Sex-reversal transgenes were generated using the Multisite Gateway Cloning System (Invitrogen). Neuron-specific promoters (amplified with primers shown in the Key Resources Table) were used to drive expression of *fem-3(+)* or *tra-2(IC)* to masculinize or feminize, respectively. Transgenic animals were generated using injection mixes, typically containing 100 ng/μl of the co-injection marker *Pelt-2::gfp* and 20–50 ng/μl of the *fem-3*, *tra-2(ic)*, or *mab-3* expression construct.

Ascarosides—Synthetic ascarosides [62] were reconstituted in 2mL EtOH and stored at −20°C. Stock ascarosides were diluted to working concentrations with Milli-Q water, aliquoted into single-use tubes, and stored at −80°C.

Behavioral Assays

Quadrant Assay: The day before the assay, L4 animals were picked to sex-segregated plates (15 animals per plate) and assay plates were prepared. A custom-made stamp was used to mark quadrant boundaries on the bottom of unseeded 6-cm NGM plates. The quadrant area comprised a 3-cm square divided into four zones with a 0.5-cm radius circle at the center. After spreading 50 μl of *E. coli* OP50 culture within the 3 cm square, plates were incubated at 20°C overnight. The day of the assay, eight 1-μL drops of ascaroside solution (either 1 μM ascr#2, 1 μM ascr#3, 10 μM ascr#8 together or 1 μM ascr#3 alone, as indicated) or control (equivalent amounts of ethanol diluted in water) were placed onto the surface of opposing pairs of quadrants (Figure 1A). At time t=0, ten worms of the appropriate sex and genotype were placed in the center circle. At t=30 min, t=60 min, and t=90 min, the number of worms in each pair of quadrants was recorded. Chemotaxis indices for the three time points [calculated as CI = (# in ascaroside quadrants – # in control)/(# in ascaroside quadrants + # in control)] were averaged together to generate a final CI value for each assay. Each CI therefore represents the behavior of ten animals over 90 minutes. Averaging three time points provides a more reliable measure of the behavior of the population; there was no evidence of adaptation to the stimulus during this time (Figure S1A). Statistical significance was assessed using the Mann-Whitney-Wilcoxon test or the Kruskal-Wallis test with Bonferroni correction and Dunn's posthoc test as described in the legends.

Male Clumping Assay: Ten young adult males were placed in the center of standard quadrant assay plates in which each quadrant contained four spots of the standard ascaroside #2/#3/#8 blend. In control experiments, assay plates contained no ascarosides. At 30 min, 60 min, and 90 min, the fraction of animals that were in contact with each other (*e.g.,* the

number of males touching at least one other male) was determined. Mann-Whitney tests were used to analyze clumping fractions at each time point.

Quadrant Assay with Immobilized Hermaphrodites: These assays were carried out using the same overall format as the *Quadrant Assay* described above. Instead of ascaroside and control solutions, genetically paralyzed *unc-13* or *unc-13; daf-22* hermaphrodites were placed in opposing quadrants (four worms per quadrant). After 30 min, ten worms of the appropriate sex and genotype were placed in the center circle ($t = 0$). Plates on which hermaphrodites moved beyond the boundaries of their quadrant (an uncommon occurrence) were censored. Preference Indices were calculated in the same manner as Chemotaxis Indices.

Mate Localization Assay (Manual): The day before the assay, L4 males were picked to individual plates and L4 *unc-13(e51)* hermaphrodites were picked to a single plate. Assay plates were prepared by spreading 10 μl of *E. coli* OP50 into a 1 cm × 2.5 cm lawn in the center of a 6-cm NGM plate and were incubated at 20°C overnight. Two hours before the start of the assay, one *unc-13* hermaphrodite was placed at one end of the bacterial lawn on each plate. The assay began when an adult male was placed at the opposing end of the lawn. All plates were checked at 5-min intervals for 60 min and the time at which the male was first observed mating with the hermaphrodite was recorded. Mating was defined by the male tail contacting the hermaphrodite and scanning for (or already at) the vulva. The fraction of males observed mating by time t was plotted. Kaplan-Meier survival curves were generated and compared using the log-rank test.

Mate Localization Assay (Video): These experiments were performed as described in *Mate Localization Assay (Manual)* above, except that the lawn size was reduced to 1 cm × 2 cm to fit smaller 3.5-cm plates, and 3 *unc-13* or *unc-13; daf-22* hermaphrodites were placed at one end of the lawn. A Basler acA2500-14um camera connected to a Fujifilm HF16Sa-1 lens was mounted above an illumination source, and Pylon Viewer software was used to capture images of the entire lawn at 1 or 2 frames/sec for 60 min. Videos were visually examined for interactions, defined as any physical contact between the male and a hermaphrodite. Mating initiation was scored as the first sustained contact that resulted in tail scanning behavior. Kaplan-Meier survival curves were generated and compared using the log-rank test with the Holm correction.

Male Mating Behavior: Male contact-response behavior was assayed by placing males on a small bacterial lawn with several immobilized hermaphrodites as described [101]. Contact response efficiency was evaluated by visual examination of the Mate Localization Assay videos. Response efficiency was calculated as the reciprocal of the number of interactions until mating initiation occurred.

Exploratory Behavior: Experiments were performed as described in *Mate Localization Assay (Video)* above except that no hermaphrodites were picked to the assay plate. Trajectories of individual males were tracked using a modified version of the Parallel Worm Tracker Matlab script [102]. Using the custom WormExploration Matlab script (see Key Resources Table), these trajectories were passed through a grid of $0.9mm^2$ squares and the

number of squares covered by each worm trajectory was determined. Statistical analysis was performed using unpaired Student's t-tests.

Neuronal calcium imaging

Automated imaging and stimulation: Neuronal imaging was performed using a Zeiss AxioObserver.A1 inverted microscope with Zeiss Plan-Apochromat objective lens (10x/0.45 NA) and a Hamamatsu Orca Flash 4.0 sCMOS camera mounted with a 1.0x C-mount adapter. MicroManager software was used to acquire image stacks (10 frames s^{-1} for 30 s per trial) and to control liquid stimulus delivery (5 – 15 s) via a microscope controller (Nobska Imaging) that actuated Parker solenoid valves via a Automate ValveLink 8.2 controller. Excitation illumination pulses (10 ms per frame) were delivered from a 50W blue LED (Mightex) or Lumencor SOLA through an EGFP filter set. For testing individual ascarosides in sequence, the inlet tube was transferred manually to each ascaroside tube and allowed to flow for 1 min between stimuli.

Microfluidic device designs: Stimulus pulses were delivered using a modified two-arena microfluidic device as previously described [46], allowing simultaneous recording from two populations. One of two stimulus streams was directed into the arenas using a computer-controlled three-way valve that switched the flow position of a "control" fluid stream, while the other stimulus stream bypassed the arena directly to the outflow. This design allowed chemical stimuli to be changed during an experiment while animals were presented a buffer solution and remained naive to the next stimulus.

Microfluidic device fabrication: Reusable monolayer microfluidic devices were prepared using soft lithography as previously described [47]. After each use, devices were cleaned in 95% EtOH at least overnight to remove residual PDMS monomers, rinsed in water and baked for at least 30 min at 65 °C to evaporate any absorbed EtOH. Devices were reversibly sealed against a hydrophobic glass slide with a support glass slide containing inlet and outlet holes drilled with a diamond-coated bit above the PDMS device and clamped in a stage adapter.

High-purity Teflon PFA tubing was used to prevent cross-contamination when presenting multiple stimuli within an experiment and for all inlet valves. Waste and animal loading connections were made with microbore tubing containing a metal tube on one end for insertion into the microfuidic device [47]. Buffers and stimuli were delivered from 30 mL syringe reservoirs, or 1.5 mL tubes when switching between stimuli in the same experiment. Fluids were delivered by hydrostatic pressure, with flowrate controlled by the distance (~70 cm) between inlet reservoirs and the outlet reservoir.

Stimulus preparation: Stimulus dilutions were prepared fresh on the day of the experiment from stock solutions of ascr#2 (1.93 mM), ascr#3 (1.41 mM), ascr#8 (0.64 mM) (all in 100% EtOH and stored at −20°C), 1X S basal kept at 20°C, and 1 M (−)-tetramisole (Sigma) in 1X S basal kept at 4°C. For all imaging experiments, dilutions were made at room temperature in 1 mM (−)-tetramisole 1X S basal buffer to paralyze body wall muscles and keep animals stationary. In experiments using ascaroside mixtures, the final stimulus

solution for imaging was a 0.1:0.1:1.0 μM mix of ascr#2:ascr#3:ascr#8 with 0.169% EtOH. Buffer and control solutions also contained 0.169% EtOH. In experiments using individual ascarosides, the stimulus solutions contained each single ascaroside at a final concentration identical to that in the ascaroside mixture with all solutions containing a final 0.169% EtOH concentration.

Experimental setup: Microfluidic arenas were assembled and degassed in a vacuum desiccator for at least 30 min before loading buffer through the outlet port. Inlet reservoirs were connected to the arena via microbore tubing [47] and the device was flushed with S basal buffer. After flow switching was verified, animals were gently injected into the arena. (In all imaging experiments, animals were tested as young adults when selected as L4s the day prior and males of a similar size.) Buffer flow continuously washed the animals, and animals were paralyzed with 1 mM tetramisole for ~1 h before recording and stimulating. After each experiment, devices were disassembled and washed to be reused as previously described [47].

Data analysis and statistics: ADF neural fluorescence was analyzed from video frames using a modified ImageJ NeuroTracker software suite and custom MATLAB scripts [46]. Background-corrected integrated neural fluorescence traces $F(t)$ were subtracted by baseline fluorescence F_0 (mean for the first 4 s) to obtain the corrected calcium response (ΔF) for each animal and stimulation trial. The peak change in neural fluorescence was quantified by finding the max ΔF between 1 second after the start and 5 seconds before the end of the stimulus pulse. Groups were compared using Kruskal-Wallis analysis and Dunn's posthoc test with Bonferroni correction. Heat maps were sorted vertically by the peak change in neural fluorescence across all individuals and repeated trials.

Because the ADF::GCaMP transgene *syEx1249* expressed GCaMP3 at very low levels, baseline fluorescence values (F_0) were close to zero. Data are reported as raw ΔF values rather than normalized $\Delta F/F_0$ to avoid excess noise and artifact. To confirm that the baseline GCaMP signal did not differ between strains, we used high-power epifluorescence microscopy to quantitate baseline fluorescence in UR1031 (wild-type background) and UR1053 (ADF-feminized) adult males. GCaMP3 fluorescence was imaged using a 40x Plan-NEOFLUAR objective on a Zeiss Axioplan 2 microscope equipped with a Hamamatsu ORCA ER camera. Fluorescence intensity was quantified using ImageJ version 1.51j as described [103]. Briefly, an outline was drawn around ADF and the area and integrated density was measured. Background fluorescence was obtained by outlining a circular area near ADF and measuring the mean fluorescence. Total Corrected Cellular Fluorescence was determined by TCCF = Integrated Density – (Area x Mean Background Fluorescence). Using this method, we obtained TCCF values for UR1031 and UR1053 of 4.54 ± 2.26 (n=13) and 4.91 ± 2.95 (n=19), respectively. An unpaired Student's t-test did not indicate that these values differed significantly (p=0.693).

QUANTIFICATION AND STATISTICAL ANALYSIS

Statistical analysis was carried out using GraphPad Prism 6 and R version 3.3.2. Most behavioral and imaging data were analyzed with non-parametric tests (Wilcoxon tests for

comparing two groups and Kruskal-Wallis analysis, followed by Dunn tests with Holm's correction, for multiple groups), obviating the need to test for normality. Unless otherwise noted, p=0.05 was used as the significance cutoff. Sample sizes were guided by those typically used in the field; however, in some cases (e.g., Figure S1b and 4f, where small effect sizes were expected), we used a power calculation to determine sample size. For quadrant assays, the chemotaxis index derived from one plate (generally containing ten tester animals) over three time points was considered one sample. Details on sample size and the nature of the statistical tests used for each experiment are given in the figure legends and in the Behavioral Assays section above.

DATA AND SOFTWARE AVAILABILITY

The Axiovision, Neurotracker, ImageJ, and Pylon Viewer software packages have been previously described and are available from the sources shown in the Key Resources Table. To obtain the data shown in Figure S5, we modified an updated version of the Parallel Worm Tracker [102] provided by J. Kubanek (Stanford University) to remove edge artifacts and reduce noise. We also wrote a new Matlab script, WormExploration, to measure worm exploratory behavior as described above. These tools are available at github.com/kfagan/ParallelWormTracker.

Supplementary Material

Refer to Web version on PubMed Central for supplementary material.

Acknowledgments

We are grateful to Denise Ferkey and Michelle Krzyzanowski for *Pelt-2::gfp* and the ADF ablation strains; to Alon Zaslaver for the *ADF::GCaMP3* transgene; and to Jan Kubanek for help with the Parallel Worm Tracker script. We thank Jagan Srinivasan for sharing unpublished data and for helpful feedback, and Ilya Ruvinsky for sharing unpublished findings. We are grateful to Clare McMahon and Kelly Rineer for contributing data to Figures S3 and 5, respectively. We thank members of the Portman lab and the Western New York Worm Group for thoughtful discussion. Some strains were provided by the *Caenorhabditis* Genetics Center, which is funded by NIH Office of Research Infrastructure Programs (P40 OD010440). This work was funded by NIH NRSA F31 NS086283 (K.F.), NSF IOS 1353075 (D.P.), NIH R01 GM108885 (D.P.), NSF CBET 1605679 (D.A.), NSF EF 1724026 (D.A.), and a Burroughs Wellcome Fund CASI Award (D.A.).

References

1. Yang CF, Shah NM. Representing sex in the brain, one module at a time. Neuron. 2014; 82:261–278. [PubMed: 24742456]
2. McCarthy MM. Multifaceted origins of sex differences in the brain. Philos Trans R Soc Lond B Biol Sci. 2016; 371:20150106. [PubMed: 26833829]
3. Auer TO, Benton R. Sexual circuitry in Drosophila. Curr Opin Neurobiol. 2016; 38:18–26. [PubMed: 26851712]
4. Garcia LR, Portman DS. Neural circuits for sexually dimorphic and sexually divergent behaviors in Caenorhabditis elegans. Curr Opin Neurobiol. 2016; 38:46–52. [PubMed: 26929998]
5. Becker, JB. Sex differences in the brain: from genes to behavior. New York: Oxford University Press; 2008.
6. Pan Y, Baker BS. Genetic identification and separation of innate and experience-dependent courtship behaviors in Drosophila. Cell. 2014; 156:236–248. [PubMed: 24439379]

7. Taylor B, Truman J. Commitment of abdominal neuroblasts in Drosophila to a male or female fate is dependent on genes of the sex-determining hierarchy. Development. 1992; 114:625–642. [PubMed: 1618132]
8. Ross JM, Kalis AK, Murphy MW, Zarkower D. The DM domain protein MAB-3 promotes sex-specific neurogenesis in C. elegans by regulating bHLH proteins. Dev Cell. 2005; 8:881–892. [PubMed: 15935777]
9. Ruta V, Datta SR, Vasconcelos ML, Freeland J, Looger LL, Axel R. A dimorphic pheromone circuit in Drosophila from sensory input to descending output. Nature. 2010; 468:686–690. [PubMed: 21124455]
10. Mellert DJ, Knapp JM, Manoli DS, Meissner GW, Baker BS. Midline crossing by gustatory receptor neuron axons is regulated by fruitless, doublesex and the Roundabout receptors. Development. 2010; 137:323–332. [PubMed: 20040498]
11. Kohl J, Ostrovsky AD, Frechter S, Jefferis GS. A bidirectional circuit switch reroutes pheromone signals in male and female brains. Cell. 2013; 155:1610–1623. [PubMed: 24360281]
12. Sammut M, Cook SJ, Nguyen KC, Felton T, Hall DH, Emmons SW, Poole RJ, Barrios A. Glia-derived neurons are required for sex-specific learning in C. elegans. Nature. 2015; 526:385–390. [PubMed: 26469050]
13. Oren-Suissa M, Bayer EA, Hobert O. Sex-specific pruning of neuronal synapses in Caenorhabditis elegans. Nature. 2016; 533:206–211. [PubMed: 27144354]
14. Simon JM, Sternberg PW. Evidence of a mate-finding cue in the hermaphrodite nematode Caenorhabditis elegans. Proceedings of the National Academy of Sciences of the United States of America. 2002; 99:1598–1603. [PubMed: 11818544]
15. White J, Nicholas T, Gritton J, Truong L, Davidson E, Jorgensen E. The sensory circuitry for sexual attraction in C. elegans males. Current biology: CB. 2007; 17:1847–1857. [PubMed: 17964166]
16. Srinivasan J, Kaplan F, Ajredini R, Zachariah C, Alborn H, Teal P, Malik R, Edison A, Sternberg P, Schroeder F. A blend of small molecules regulates both mating and development in Caenorhabditis elegans. Nature. 2008; 454:1115–1118. [PubMed: 18650807]
17. Pungaliya C, Srinivasan J, Fox BW, Malik RU, Ludewig AH, Sternberg PW, Schroeder FC. A shortcut to identifying small molecule signals that regulate behavior and development in Caenorhabditis elegans. Proceedings of the National Academy of Sciences of the United States of America. 2009; 106:7708–7713. [PubMed: 19346493]
18. Leighton DH, Choe A, Wu SY, Sternberg PW. Communication between oocytes and somatic cells regulates volatile pheromone production in Caenorhabditis elegans. Proceedings of the National Academy of Sciences of the United States of America. 2014; 111:17905–17910. [PubMed: 25453110]
19. Ludewig, AH., Schroeder, FC. WormBook: the online review of C. elegans biology. 2013. Ascaroside signaling in C. elegans; p. 1-22.
20. Jang H, Kim K, Neal SJ, Macosko E, Kim D, Butcher RA, Zeiger DM, Bargmann CI, Sengupta P. Neuromodulatory state and sex specify alternative behaviors through antagonistic synaptic pathways in C. elegans. Neuron. 2012; 75:585–592. [PubMed: 22920251]
21. Izrayelit Y, Srinivasan J, Campbell SL, Jo Y, von Reuss SH, Genoff MC, Sternberg PW, Schroeder FC. Targeted metabolomics reveals a male pheromone and sex-specific ascaroside biosynthesis in Caenorhabditis elegans. ACS chemical biology. 2012; 7:1321–1325. [PubMed: 22662967]
22. Macosko EZ, Pokala N, Feinberg EH, Chalasani SH, Butcher RA, Clardy J, Bargmann CI. A hub-and-spoke circuit drives pheromone attraction and social behaviour in C. elegans. Nature. 2009; 458:1171–1175. [PubMed: 19349961]
23. Fenk LA, de Bono M. Memory of recent oxygen experience switches pheromone valence in Caenorhabditis elegans. Proceedings of the National Academy of Sciences of the United States of America. 2017; 114:4195–4200. [PubMed: 28373553]
24. Narayan A, Venkatachalam V, Durak O, Reilly DK, Bose N, Schroeder FC, Samuel AD, Srinivasan J, Sternberg PW. Contrasting responses within a single neuron class enable sex-specific attraction in Caenorhabditis elegans. Proceedings of the National Academy of Sciences of the United States of America. 2016; 113:E1392–1401. [PubMed: 26903633]

25. Barr MM, García LR, Portman DS. Sexual dimorphism and sex differences in C. elegans neuronal development and behavior. Genetics. 2017 in press.
26. Wolff JR, Zarkower D. Somatic sexual differentiation in Caenorhabditis elegans. Current topics in developmental biology. 2008; 83:1–39. [PubMed: 19118662]
27. Kopp A. Dmrt genes in the development and evolution of sexual dimorphism. Trends Genet. 2012; 28:175–184. [PubMed: 22425532]
28. Matson CK, Zarkower D. Sex and the singular DM domain: insights into sexual regulation, evolution and plasticity. Nature reviews Genetics. 2012; 13:163–174.
29. Shen MM, Hodgkin J. mab-3, a gene required for sex-specific yolk protein expression and a male-specific lineage in C. elegans. Cell. 1988; 54:1019–1031. [PubMed: 3046751]
30. Yi W, Ross JM, Zarkower D. *mab-3* is a direct *tra-1* target gene regulating diverse aspects of *C. elegans* male sexual development and behavior. Development. 2000; 127:4469–4480. [PubMed: 11003845]
31. Lints R, Emmons SW. Regulation of sex-specific differentiation and mating behavior in *C. elegans* by a new member of the DM domain transcription factor family. Genes Dev. 2002; 16:2390–2402. [PubMed: 12231628]
32. Siehr MS, Koo PK, Sherlekar AL, Bian X, Bunkers MR, Miller RM, Portman DS, Lints R. Multiple doublesex-related genes specify critical cell fates in a C. elegans male neural circuit. PloS one. 2011; 6:e26811. [PubMed: 22069471]
33. Serrano-Saiz E, Oren-Suissa M, Bayer EA, Hobert O. Sexually Dimorphic Differentiation of a C. elegans Hub Neuron Is Cell Autonomously Controlled by a Conserved Transcription Factor. Current biology: CB. 2017; 27:199–209. [PubMed: 28065609]
34. Lee K, Portman D. Neural sex modifies the function of a C. elegans sensory circuit. Current biology: CB. 2007; 17:1858–1863. [PubMed: 17964163]
35. Mowrey WR, Bennett JR, Portman DS. Distributed Effects of Biological Sex Define Sex-Typical Motor Behavior in Caenorhabditis elegans. The Journal of neuroscience: the official journal of the Society for Neuroscience. 2014; 34:1579–1591. [PubMed: 24478342]
36. Ryan DA, Miller RM, Lee K, Neal SJ, Fagan KA, Sengupta P, Portman DS. Sex, age, and hunger regulate behavioral prioritization through dynamic modulation of chemoreceptor expression. Current biology: CB. 2014; 24:2509–2517. [PubMed: 25438941]
37. Hilbert ZA, Kim DH. Sexually dimorphic control of gene expression in sensory neurons regulates decision-making behavior in C. elegans. Elife. 2017; 6
38. Portman DS. Sexual modulation of sex-shared neurons and circuits in Caenorhabditis elegans. J Neurosci Res. 2017; 95:527–538. [PubMed: 27870393]
39. Peden E, Kimberly E, Gengyo-Ando K, Mitani S, Xue D. Control of sex-specific apoptosis in C. elegans by the BarH homeodomain protein CEH-30 and the transcriptional repressor UNC-37/Groucho. Genes Dev. 2007; 21:3195–3207. [PubMed: 18056429]
40. Schwartz H, Horvitz H. The C. elegans protein CEH-30 protects male-specific neurons from apoptosis independently of the Bcl-2 homolog CED-9. Genes Dev. 2007; 21:3181–3194. [PubMed: 18056428]
41. Mehra A, Gaudet J, Heck L, Kuwabara PE, Spence AM. Negative regulation of male development in Caenorhabditis elegans by a protein-protein interaction between TRA-2A and FEM-3. Genes Dev. 1999; 13:1453–1463. [PubMed: 10364161]
42. Bae Y, Barr M. Sensory roles of neuronal cilia: cilia development, morphogenesis, and function in C. elegans. Front Biosci. 2008; 13:5959–5974. [PubMed: 18508635]
43. Bargmann CI, Horvitz HR. Control of larval development by chemosensory neurons in Caenorhabditis elegans. Science. 1991; 251:1243–1246. [PubMed: 2006412]
44. Krzyzanowski MC, Woldemariam S, Wood JF, Chaubey AH, Brueggemann C, Bowitch A, Bethke M, L'Etoile ND, Ferkey DM. Aversive Behavior in the Nematode C. elegans Is Modulated by cGMP and a Neuronal Gap Junction Network. PLoS genetics. 2016; 12:e1006153. [PubMed: 27459302]
45. Chelur DS, Chalfie M. Targeted cell killing by reconstituted caspases. Proceedings of the National Academy of Sciences of the United States of America. 2007; 104:2283–2288. [PubMed: 17283333]

46. Larsch J, Ventimiglia D, Bargmann CI, Albrecht DR. High-throughput imaging of neuronal activity in Caenorhabditis elegans. Proceedings of the National Academy of Sciences of the United States of America. 2013; 110:E4266–4273. [PubMed: 24145415]
47. Lagoy RC, Albrecht DR. Microfluidic Devices for Behavioral Analysis, Microscopy, and Neuronal Imaging in Caenorhabditis elegans. Methods Mol Biol. 2015; 1327:159–179. [PubMed: 26423974]
48. Richmond J, Davis W, Jorgensen E. UNC-13 is required for synaptic vesicle fusion in C. elegans. Nature neuroscience. 1999; 2:959–964. [PubMed: 10526333]
49. White JG, Southgate E, Thomson JN, Brenner S. The structure of the nervous system of the nematode *Caenorhabditis elegans*. Phil Trans R Soc Lond B. 1986; 314:1–340. [PubMed: 22462104]
50. Kim K, Sato K, Shibuya M, Zeiger DM, Butcher RA, Ragains JR, Clardy J, Touhara K, Sengupta P. Two chemoreceptors mediate developmental effects of dauer pheromone in C. elegans. Science. 2009; 326:994–998. [PubMed: 19797623]
51. McGrath PT, Xu Y, Ailion M, Garrison JL, Butcher RA, Bargmann CI. Parallel evolution of domesticated Caenorhabditis species targets pheromone receptor genes. Nature. 2011; 477:321–325. [PubMed: 21849976]
52. Park D, O'Doherty I, Somvanshi RK, Bethke A, Schroeder FC, Kumar U, Riddle DL. Interaction of structure-specific and promiscuous G-protein-coupled receptors mediates small-molecule signaling in Caenorhabditis elegans. Proceedings of the National Academy of Sciences of the United States of America. 2012; 109:9917–9922. [PubMed: 22665789]
53. Greene JS, Dobosiewicz M, Butcher RA, McGrath PT, Bargmann CI. Regulatory changes in two chemoreceptor genes contribute to a Caenorhabditis elegans QTL for foraging behavior. Elife. 2016; 5
54. Greene JS, Brown M, Dobosiewicz M, Ishida IG, Macosko EZ, Zhang X, Butcher RA, Cline DJ, McGrath PT, Bargmann CI. Balancing selection shapes density-dependent foraging behaviour. Nature. 2016; 539:254–258. [PubMed: 27799655]
55. Troemel ER, Chou JH, Dwyer ND, Colbert HA, Bargmann CI. Divergent seven transmembrane receptors are candidate chemosensory receptors in *C. elegans*. Cell. 1995; 83:207–218. [PubMed: 7585938]
56. Raymond CS, Shamu CE, Shen MM, Seifert KJ, Hirsch B, Hodgkin J, Zarkower D. Evidence for evolutionary conservation of sex-determining genes. Nature. 1998; 391:691–695. [PubMed: 9490411]
57. Mason D, Rabinowitz J, Portman D. dmd-3, a doublesex-related gene regulated by tra-1, governs sex-specific morphogenesis in C. elegans. Development. 2008; 135:2373–2382. [PubMed: 18550714]
58. Aprison EZ, Ruvinsky I. Counteracting Ascarosides Act through Distinct Neurons to Determine the Sexual Identity of C. elegans Pheromones. Current biology: CB. 2017; 27:2589–2599. e2583. [PubMed: 28844646]
59. von Reuss SH, Bose N, Srinivasan J, Yim JJ, Judkins JC, Sternberg PW, Schroeder FC. Comparative metabolomics reveals biogenesis of ascarosides, a modular library of small-molecule signals in C. elegans. J Am Chem Soc. 2012; 134:1817–1824. [PubMed: 22239548]
60. Kaplan F, Srinivasan J, Mahanti P, Ajredini R, Durak O, Nimalendran R, Sternberg PW, Teal PE, Schroeder FC, Edison AS, et al. Ascaroside expression in Caenorhabditis elegans is strongly dependent on diet and developmental stage. PloS one. 2011; 6:e17804. [PubMed: 21423575]
61. Zhang X, Li K, Jones RA, Bruner SD, Butcher RA. Structural characterization of acyl-CoA oxidases reveals a direct link between pheromone biosynthesis and metabolic state in Caenorhabditis elegans. Proceedings of the National Academy of Sciences of the United States of America. 2016; 113:10055–10060. [PubMed: 27551084]
62. Butcher RA, Fujita M, Schroeder FC, Clardy J. Small-molecule pheromones that control dauer development in Caenorhabditis elegans. Nature chemical biology. 2007; 3:420–422. [PubMed: 17558398]
63. Golden JW, Riddle DL. A gene affecting production of the Caenorhabditis elegans dauer-inducing pheromone. Mol Gen Genet. 1985; 198:534–536. [PubMed: 3859733]

64. Gomez-Diaz C, Benton R. The joy of sex pheromones. EMBO Rep. 2013; 14:874–883. [PubMed: 24030282]

65. Sze JY, Victor M, Loer C, Shi Y, Ruvkun G. Food and metabolic signalling defects in a *Caenorhabditis elegans* serotonin-synthesis mutant. Nature. 2000; 403:560–564. [PubMed: 10676966]

66. Iwanir S, Brown AS, Nagy S, Najjar D, Kazakov A, Lee KS, Zaslaver A, Levine E, Biron D. Serotonin promotes exploitation in complex environments by accelerating decision-making. BMC biology. 2016; 14:9. [PubMed: 26847342]

67. Zaslaver A, Liani I, Shtangel O, Ginzburg S, Yee L, Sternberg PW. Hierarchical sparse coding in the sensory system of Caenorhabditis elegans. Proceedings of the National Academy of Sciences of the United States of America. 2015; 112:1185–1189. [PubMed: 25583501]

68. Sawin ER, Ranganathan R, Horvitz HR. C. elegans locomotory rate is modulated by the environment through a dopaminergic pathway and by experience through a serotonergic pathway. Neuron. 2000; 26:619–631. [PubMed: 10896158]

69. Mowrey WR, Portman DS. Sex differences in behavioral decision-making and the modulation of shared neural circuits. Biology of sex differences. 2012; 3:8. [PubMed: 22436578]

70. McCarthy MM, Arnold AP, Ball GF, Blaustein JD, De Vries GJ. Sex differences in the brain: the not so inconvenient truth. The Journal of neuroscience: the official journal of the Society for Neuroscience. 2012; 32:2241–2247. [PubMed: 22396398]

71. Siwicki KK, Kravitz EA. Fruitless, doublesex and the genetics of social behavior in Drosophila melanogaster. Curr Opin Neurobiol. 2009; 19:200–206. [PubMed: 19541474]

72. Clyne JD, Miesenböck G. Sex-specific control and tuning of the pattern generator for courtship song in Drosophila. Cell. 2008; 133:354–363. [PubMed: 18423205]

73. Kimchi T, Xu J, Dulac C. A functional circuit underlying male sexual behaviour in the female mouse brain. Nature. 2007; 448:1009–1014. [PubMed: 17676034]

74. Rezaval C, Pattnaik S, Pavlou HJ, Nojima T, Bruggemeier B, D'Souza LA, Dweck HK, Goodwin SF. Activation of Latent Courtship Circuitry in the Brain of Drosophila Females Induces Male-like Behaviors. Current biology: CB. 2016; 26:2508–2515. [PubMed: 27568592]

75. Datta S, Vasconcelos M, Ruta V, Luo S, Wong A, Demir E, Flores J, Balonze K, Dickson B, Axel R. The Drosophila pheromone cVA activates a sexually dimorphic neural circuit. Nature. 2008; 452:473–477. [PubMed: 18305480]

76. Nayak SV, Singh RN. Sensilla on the Tarsal Segments and Mouthparts of Adult Drosophila-Melanogaster Meigen (Diptera, Drosophilidae). Int J Insect Morphol. 1983; 12:273–291.

77. Possidente DR, Murphey RK. Genetic control of sexually dimorphic axon morphology in Drosophila sensory neurons. Developmental biology. 1989; 132:448–457. [PubMed: 2924997]

78. Schneiderman AM, Hildebrand JG, Brennan MM, Tumlinson JH. Transsexually grafted antennae alter pheromone-directed behaviour in a moth. Nature. 1986; 323:801–803. [PubMed: 3774007]

79. White JQ, Jorgensen EM. Sensation in a single neuron pair represses male behavior in hermaphrodites. Neuron. 2012; 75:593–600. [PubMed: 22920252]

80. Gruner M, Nelson D, Winbush A, Hintz R, Ryu L, Chung SH, Kim K, Gabel CV, van der Linden AM. Feeding state, insulin and NPR-1 modulate chemoreceptor gene expression via integration of sensory and circuit inputs. PLoS genetics. 2014; 10:e1004707. [PubMed: 25357003]

81. Hale LA, Lee ES, Pantazis AK, Chronis N, Chalasani SH. Altered Sensory Code Drives Juvenile-to-Adult Behavioral Maturation in Caenorhabditis elegans. eNeuro. 2016; 3

82. Fujiwara M, Aoyama I, Hino T, Teramoto T, Ishihara T. Gonadal Maturation Changes Chemotaxis Behavior and Neural Processing in the Olfactory Circuit of Caenorhabditis elegans. Current biology: CB. 2016; 26:1522–1531. [PubMed: 27265391]

83. Oda S, Toyoshima Y, de Bono M. Modulation of sensory information processing by a neuroglobin in Caenorhabditis elegans. Proceedings of the National Academy of Sciences of the United States of America. 2017; 114:E4658–E4665. [PubMed: 28536200]

84. Ghosh DD, Sanders T, Hong S, McCurdy LY, Chase DL, Cohen N, Koelle MR, Nitabach MN. Neural Architecture of Hunger-Dependent Multisensory Decision Making in C. elegans. Neuron. 2016; 92:1049–1062. [PubMed: 27866800]

85. Zahratka JA, Williams PD, Summers PJ, Komuniecki RW, Bamber BA. Serotonin differentially modulates Ca2+ transients and depolarization in a C. elegans nociceptor. Journal of neurophysiology. 2015; 113:1041–1050. [PubMed: 25411461]

86. Harris GP, Hapiak VM, Wragg RT, Miller SB, Hughes LJ, Hobson RJ, Steven R, Bamber B, Komuniecki RW. Three distinct amine receptors operating at different levels within the locomotory circuit are each essential for the serotonergic modulation of chemosensation in Caenorhabditis elegans. The Journal of neuroscience: the official journal of the Society for Neuroscience. 2009; 29:1446–1456. [PubMed: 19193891]

87. Ezcurra M, Tanizawa Y, Swoboda P, Schafer WR. Food sensitizes C. elegans avoidance behaviours through acute dopamine signalling. The EMBO journal. 2011; 30:1110–1122. [PubMed: 21304491]

88. Ohno H, Sakai N, Adachi T, Iino Y. Dynamics of Presynaptic Diacylglycerol in a Sensory Neuron Encode Differences between Past and Current Stimulus Intensity. Cell Rep. 2017; 20:2294–2303. [PubMed: 28877465]

89. Kobayashi K, Nakano S, Amano M, Tsuboi D, Nishioka T, Ikeda S, Yokoyama G, Kaibuchi K, Mori I. Single-Cell Memory Regulates a Neural Circuit for Sensory Behavior. Cell Rep. 2016; 14:11–21. [PubMed: 26725111]

90. Claudianos C, Lim J, Young M, Yan S, Cristino AS, Newcomb RD, Gunasekaran N, Reinhard J. Odor memories regulate olfactory receptor expression in the sensory periphery. Eur J Neurosci. 2014; 39:1642–1654. [PubMed: 24628891]

91. Root CM, Ko KI, Jafari A, Wang JW. Presynaptic facilitation by neuropeptide signaling mediates odor-driven food search. Cell. 2011; 145:133–144. [PubMed: 21458672]

92. Tong J, Mannea E, Aime P, Pfluger PT, Yi CX, Castaneda TR, Davis HW, Ren X, Pixley S, Benoit S, et al. Ghrelin enhances olfactory sensitivity and exploratory sniffing in rodents and humans. The Journal of neuroscience: the official journal of the Society for Neuroscience. 2011; 31:5841–5846. [PubMed: 21490225]

93. Savigner A, Duchamp-Viret P, Grosmaitre X, Chaput M, Garcia S, Ma M, Palouzier-Paulignan B. Modulation of spontaneous and odorant-evoked activity of rat olfactory sensory neurons by two anorectic peptides, insulin and leptin. Journal of neurophysiology. 2009; 101:2898–2906. [PubMed: 19297511]

94. Dey S, Chamero P, Pru JK, Chien MS, Ibarra-Soria X, Spencer KR, Logan DW, Matsunami H, Peluso JJ, Stowers L. Cyclic Regulation of Sensory Perception by a Female Hormone Alters Behavior. Cell. 2015; 161:1334–1344. [PubMed: 26046438]

95. Bargmann CI. Beyond the connectome: How neuromodulators shape neural circuits. BioEssays: news and reviews in molecular, cellular and developmental biology. 2012; 34:458–465.

96. Marder E. Neuromodulation of neuronal circuits: back to the future. Neuron. 2012; 76:1–11. [PubMed: 23040802]

97. Kirszenblat L, van Swinderen B. The Yin and Yang of Sleep and Attention. Trends in neurosciences. 2015; 38:776–786. [PubMed: 26602764]

98. Kim SM, Su CY, Wang JW. Neuromodulation of Innate Behaviors in Drosophila. Annu Rev Neurosci. 2017; 40:327–348. [PubMed: 28441115]

99. Trojanowski NF, Raizen DM. Call it Worm Sleep. Trends in neurosciences. 2016; 39:54–62. [PubMed: 26747654]

100. Brenner S. The genetics of *Caenorhabditis elegans*. Genetics. 1974; 77:71–94. [PubMed: 4366476]

101. Morsci NS, Haas LA, Barr MM. Sperm status regulates sexual attraction in Caenorhabditis elegans. Genetics. 2011; 189:1341–1346. [PubMed: 21968192]

102. Ramot D, Johnson BE, Berry TL Jr, Carnell L, Goodman MB. The Parallel Worm Tracker: a platform for measuring average speed and drug-induced paralysis in nematodes. PloS one. 2008; 3:e2208. [PubMed: 18493300]

103. McCloy RA, Rogers S, Caldon CE, Lorca T, Castro A, Burgess A. Partial inhibition of Cdk1 in G 2 phase overrides the SAC and decouples mitotic events. Cell Cycle. 2014; 13:1400–1412. [PubMed: 24626186]

104. Larsch J, Flavell SW, Liu Q, Gordus A, Albrecht DR, Bargmann CI. A Circuit for Gradient Climbing in C. elegans Chemotaxis. Cell Rep. 2015; 12:1748–1760. [PubMed: 26365196]

105. Schneider CA, Rasband WS, Eliceiri KW. NIH Image to ImageJ: 25 years of image analysis. Nat Methods. 2012; 9:671–675. [PubMed: 22930834]

HIGHLIGHTS

- The sex of the ADF neurons determines the valence of the response to sex pheromones
- ADF detects pheromone only in males, overcoming non-sex-specific repulsion
- The *doublesex* ortholog *mab-3* couples the genetic sex of ADF to its male state
- Sex specific tuning of ADF is necessary for males to use pheromones to locate mates

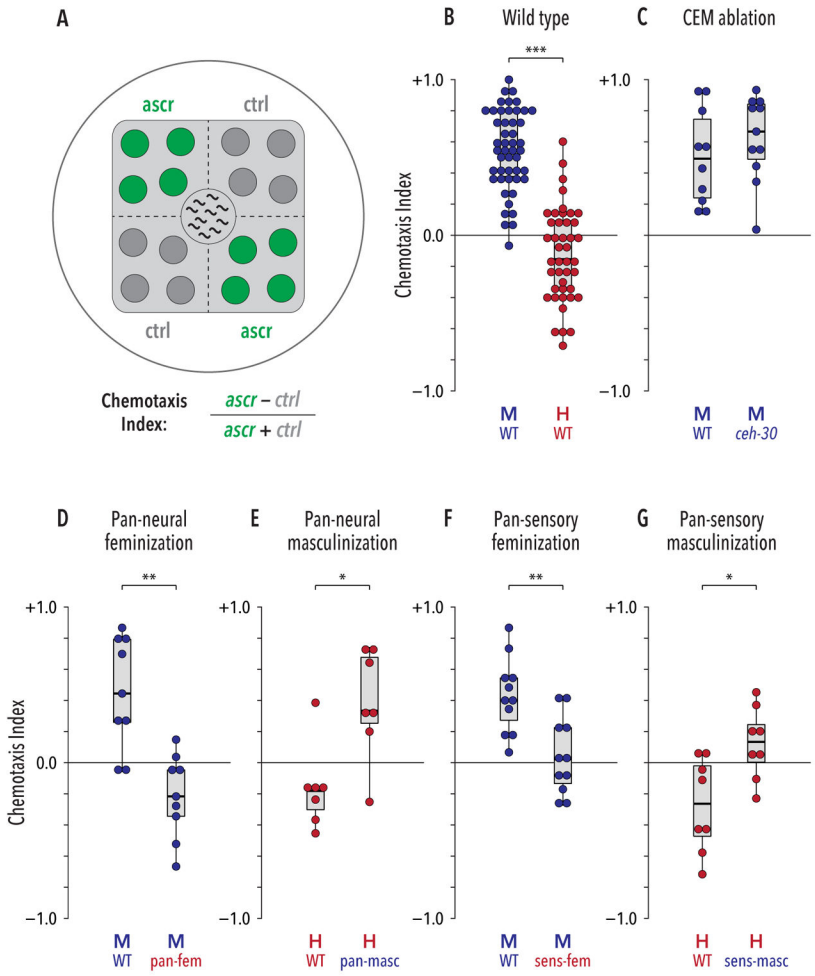

Figure 1. Sexual modulation of shared circuits generates sexually dimorphic behavioral responses to ascarosides

(A) Ascaroside quadrant assay. 1-μL drops of ascaroside or control solutions (green and dark gray, respectively) were spotted on opposite quadrants of a standard culture plate with a square lawn of bacterial food (light gray). Ten animals were placed at the center and their positions were scored at regular intervals to derive a Chemotaxis Index (see STAR Methods). (B) Wild-type animals showed a marked sex difference in behavioral responses to the ascr#2/#3/#8 mixture: males were strongly attracted, while hermaphrodites were weakly repelled. (C) Loss of CEM neurons (*ceh-30(lf)* mutants) did not detectably influence male behavior. (D, E) Pan-neural feminization ("pan-fem") caused pheromone repulsion in males, while pan-neural masculinization ("pan-masc") generated marked attraction in hermaphrodites. (F, G) Feminization of all ciliated sensory neurons ("sens-fem") eliminated ascaroside attraction in males. Masculinization of ciliated sensory neurons ("sens-masc") caused a significant change in behavior in hermaphrodites. *$p \leq 0.05$, **$p \leq 0.01$, ***$p \leq 0.001$ by Mann-Whitney test. See also Figure S1.

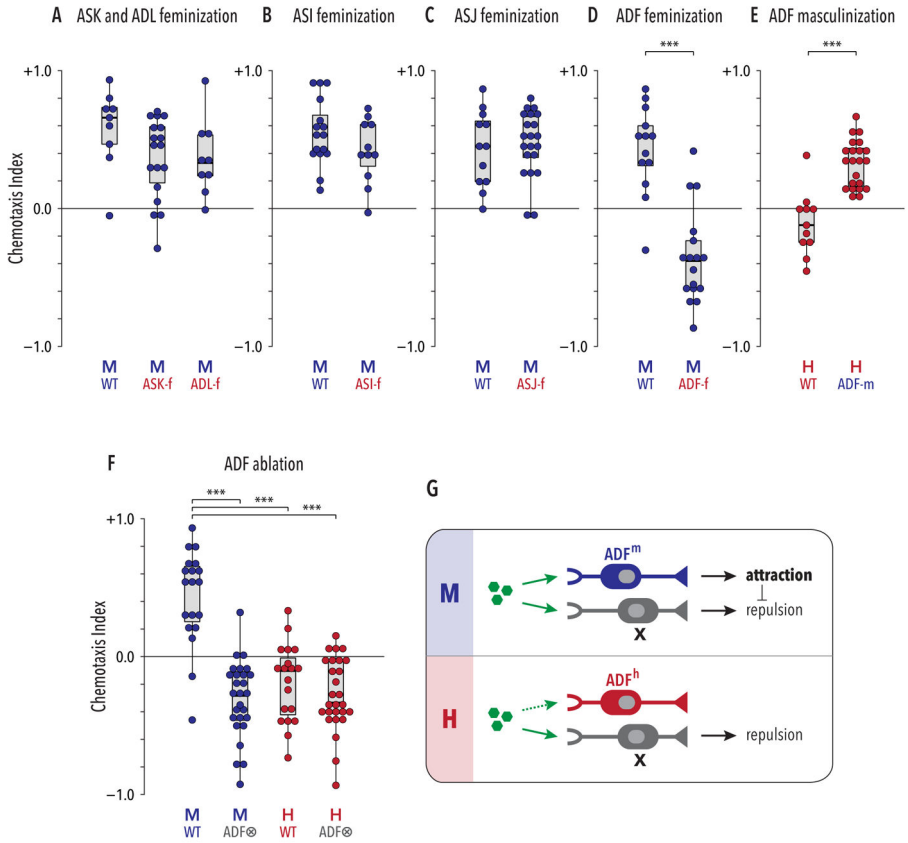

Figure 2. The genetic sex of the ADF sensory neuron pair determines the valence of the behavioral response to ascaroside pheromones

(A–C) Genetic feminization of the ASK, ADL, ASI, or ASJ neurons (indicated by "*neuron name*-f") did not have pronounced effects on male ascaroside attraction. As we have no convenient means to assess whether these transgenes successfully altered the sexual state of these cells, these results do not rule out a role for genetic sex. (D) ADF-specific feminization ("ADF-f") reversed the valence of males' response to ascarosides, converting attraction to repulsion. (E) ADF-specific masculinization in hermaphrodites ("ADF-m") converted repulsion into attraction. (F) Genetic ablation of ADF ("ADF⊗") eliminated sex differences in pheromone response behavior. ADF-ablated animals of both sexes were weakly repelled by ascarosides. (G) Model: ADF sex determines behavioral valence by promoting pheromone attraction in males and inhibiting a non-sex-specific repulsive drive. In both sexes, an unknown neuronal activity, neuron X (likely ADL [20]; see Discussion), promotes repulsion from ascarosides (green hexagons). In its male state (ADF^m; upper panel), ADF promotes ascaroside attraction, overcoming X's repulsive influence. In its hermaphrodite state (ADF^f; lower panel), ADF has no apparent role in this behavior, allowing the activity of X to prevail. In (A) and (F), groups were compared with Kruskal-Wallis analysis followed by Dunn tests with Holm's correction. In (B–E), Mann-Whitney tests were used. ***$p \leq 0.001$. See also Figure S2.

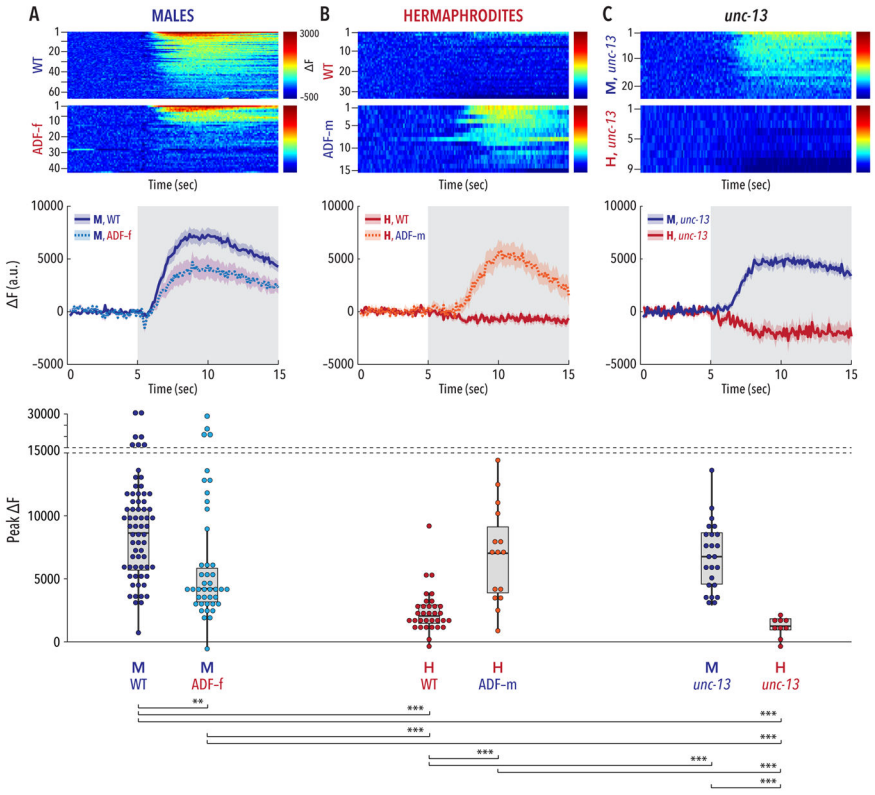

Figure 3. The sexual state of ADF governs its ability to respond to ascaroside stimulation

Upper panels show pseudocolored graphs of calcium recordings of individual neuronal responses to stimulation with an ascr#2/#3/#8 mixture. Each animal underwent three rounds of stimulation; each row depicts a single response, sorted by peak activity. The pseudocolor scale represents GCaMP3 ΔF (red highest, blue lowest). *Middle panels* show average ΔF intensities ± SEM for the recordings depicted in the upper panels. Gray shading indicates the period of ascaroside stimulation. *Lower panels* show peak ΔF values for each recording; dots represent individual responses to each pulse. (A) Wild-type males showed robust calcium transients in ADF upon ascaroside stimulation. The strength of this response was significantly reduced in ADF-feminized males. The modest reduction in mean response (central panel) likely reflects a bimodal distribution of responses arising from variable effects of the ADF feminization transgene, more clearly apparent in the lower panel. (B) In wild-type hermaphrodites, ADF appeared insensitive to ascaroside stimulation. Masculinization of ADF in an otherwise wild-type hermaphrodite was sufficient to confer robust ascaroside sensitivity to ADF. (C) *unc-13* mutants maintained a marked sex difference in the response of ADF to ascaroside stimulation. $n = 9–66$ trials (3–22 animals with 3 trials per animal). Groupwise comparison of peak ΔF values was carried out using Kruskal-Wallis analysis and Dunn's posthoc test with Bonferroni correction. $^{**}p \leq 0.01$, $^{***}p \leq 0.001$. See also Figure S3.

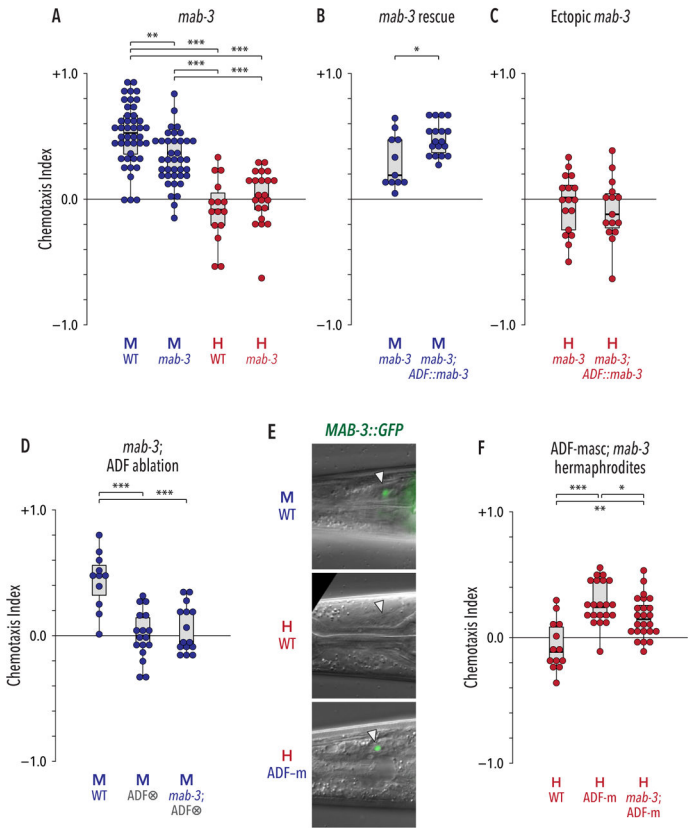

Figure 4. The *doublesex* ortholog *mab-3* acts downstream of *tra-1* to cell-autonomously promote the male state of ADF

(A) *mab-3* mutant males had a reduced preference for ascr#3 compared to WT males, but loss of *mab-3* had no detectable effect on hermaphrodite behavior. (B) ADF-specific expression of *mab-3(+)* ("*ADF::mab-3*") rescued the behavioral defect of *mab-3* males. (C) ADF-specific expression of *mab-3(+)* in hermaphrodites was not sufficient to generate pheromone attraction. (D) Loss of *mab-3* did not further disrupt ascr#3 response when ADF was ablated. (E) *MAB-3::GFP* was expressed in ADF (white triangles) in WT adult males, but not in WT adult hermaphrodites. Genetic feminization of ADF was sufficient to activate ADF in hermaphrodites. (F) The effect of ADF masculinization on hermaphrodite behavior partially requires *mab-3* function. All experiments in this figure were carried out with ascr#3 alone. In (A), (D), and (F), data were analyzed by Kruskal-Wallis tests followed by Dunn tests with Holm's correction. In (B) and (C), Mann-Whitney tests were used. *$p \leq 0.05$, **$p \leq 0.01$, ***$p \leq 0.001$. See also Figure S4.

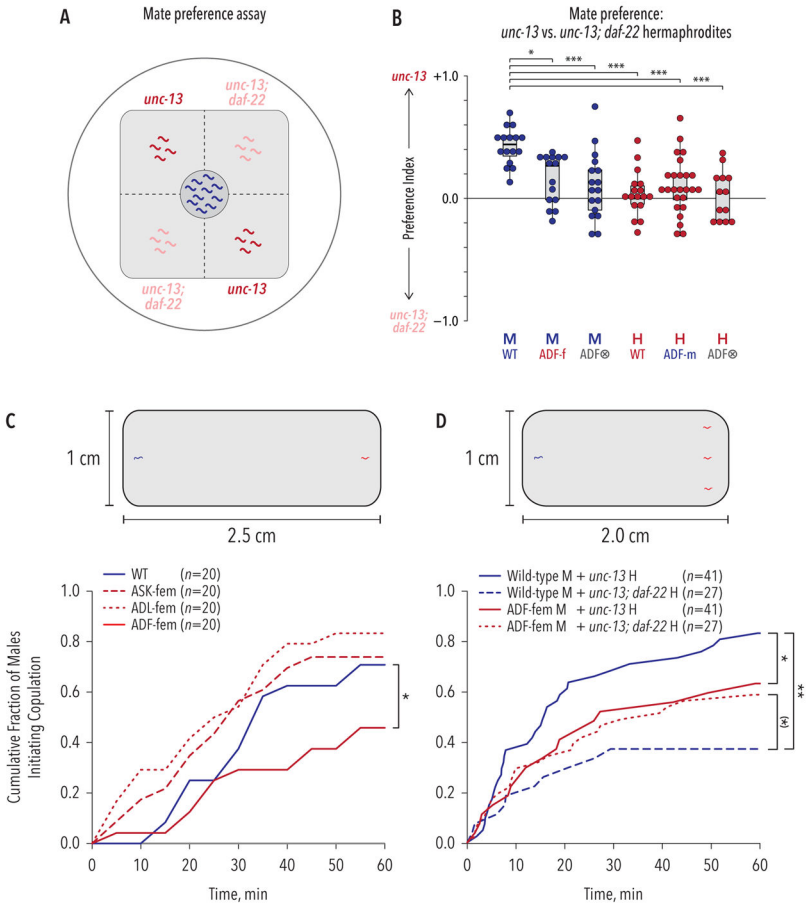

Figure 5. Male-specific tuning of ADF is necessary for males to use ascarosides to locate mates

(A) A modified quadrant assay was used to measure the ability of males to distinguish between immobilized ascaroside-producing (*unc-13*, red) and ascaroside-lacking (*unc-13; daf-22*, pink) hermaphrodites. (B) Wild-type males exhibited a marked preference for associating with ascaroside-producing over ascaroside-lacking hermaphrodites, while wild-type hermaphrodites showed no bias toward either. ADF feminization reduced this preference in males, and ADF ablation nearly eliminated it. Neither ADF masculinization nor ADF ablation had noticeable effects in hermaphrodites. Kruskal-Wallis analysis with Holm-corrected Dunn's tests were used to assess significance. (C, D) Male mate-searching assays. *Upper,* diagrams of assay conditions. Gray regions represent lawns of *E. coli*. The starting points of males (blue) and hermaphrodites (red) are shown. *Lower,* cumulative rates with which males locate and initiate copulation with hermaphrodites. (C) Compared to wild-type males (blue line), feminization of ADF (solid red line) compromised the ability of males to locate and copulate with hermaphrodites. Feminization of ASK or ADL (dashed or dotted red lines) had no detectable effect. (D) Wild-type males took longer to find and copulate with *daf-22* hermaphrodites (dashed blue line) compared to wild-type hermaphrodites (solid blue line). Feminization of ADF (solid red line) impaired males' ability to find mates; it also eliminated the ability of males to use hermaphrodite-produced ascarosides as mate-location cues (compare solid red to dashed red lines). In (C) and (D), Kaplan-Meier survival curves were generated and compared using log-rank tests with the

Holm correction. Numbers of males assayed n is shown in the figure. $^{(*)}p = 0.093$, $^{*}p \leq 0.05$, $^{**}p \leq 0.01$, $^{***}p \leq 0.001$. See also Figure S5.

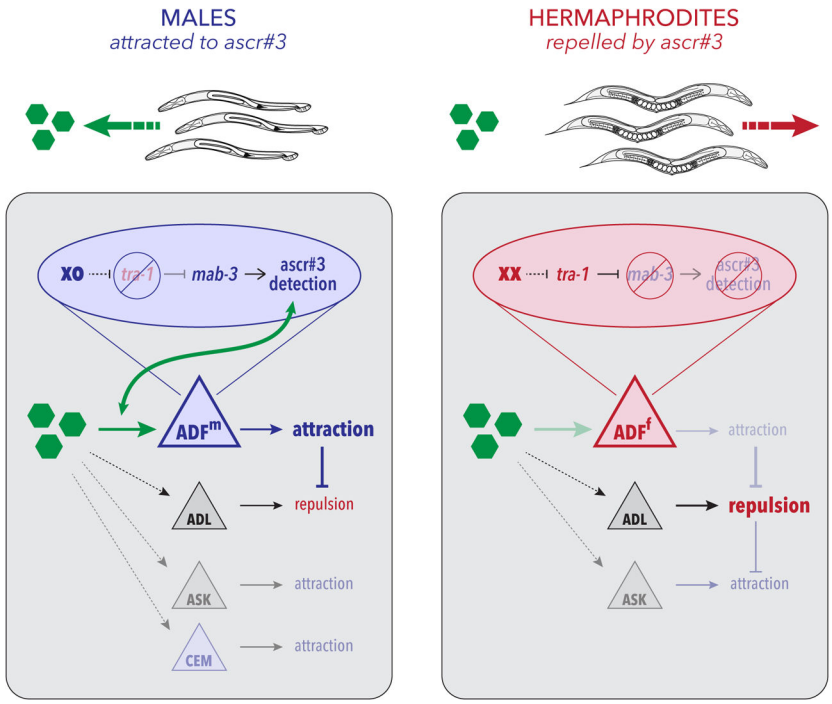

Figure 6. The genetic sex of ADF acts through *mab-3* to control a chemosensory switch that determines the valence of ascaroside response behavior

Green hexagons depict ascaroside pheromones; triangles represent sensory neurons. Blue triangles indicate the male state of the shared neuron ADF (ADF^m) and the male-specific CEM neurons. The red triangle indicates the hermaphrodite state of ADF (ADF^h). Gray triangles depict shared neurons in which genetic sex does not appear to have a prominent role. Blue and red ovals show the genetic mechanism that links chromosomal sex to the regulation of ascaroside detection by ADF in its male and hermaphrodite states, respectively. In males, genetic sex acts through *mab-3* to confer the ability to detect ascarosides onto ADF. In turn, this likely engages shared circuitry to promote attraction, overcoming a non-sex-specific repulsion to ascarosides, likely generated by ADL. In other behavioral contexts, the ASK and CEM neurons promote ascaroside attraction, though their roles in the assay used here appear to be secondary. In hermaphrodites, *tra-1* represses *mab-3*, preventing ADF from detecting ascaroside stimuli and allowing repulsion, likely driven by ADL, to prevail.

KEY RESOURCES TABLE

REAGENT or RESOURCE	SOURCE	IDENTIFIER
Bacterial and Virus Strains		
E. coli OP50	*Caenorhabditis* genetics center	
Chemicals, Peptides, and Recombinant Proteins		
Synthetic ascarosides (ascr#2, #3, #8)	Synthesized by F. Schroeder laboratory, Boyce Thompson Institute, Ithaca, NY	
Experimental Models: Organisms/Strains		
C. elegans strain: *pkd-2(sy606) IV; him-5(e1490) V*	*Caenorhabditis* Genetics Center	PT8
C. elegans strain: *him-5(e1490) V; fsEx160[Posm-5::fem-3(+)::SL2::mCherry, Punc-122::GFP]*	[35]	UR226
C. elegans strain: *him-5(e1490) V; fsIs15[Prab-3::fem-3(+)::SL2::mCherry; Punc-122::GFP]*	[36]	UR236
C. elegans strain: *mab-3(e2093) II; him-5(e1490) V*	*Caenorhabditis* Genetics Center; this paper	UR278
C. elegans strain: *him-5(e1490) V; fsEx357[Posm-5::tra-2(ic)::SL2::mCherry]*	This paper	UR754
C. elegans strain: *him-5(e1490) V; fsEx317[Prab-3::tra-2(ic)::SL2::mCherry; Punc-122::GFP]*	This paper	UR866
C. elegans strain: *him-5(e1490) V*	*Caenorhabditis* Genetics Center; this paper	UR926
C. elegans strain: *him-5(e1490) V; fsEx449 [Psrh-142::tra-2(ic)::SL2::mCherry; Pelt-2::GFP line 1]*	This paper	UR940
C. elegans strain: *him-5(e1490) V; fsEx454 [Pgpa-4::tra-2(ic)::SL2::mCherry; Pelt-2::GFP line 1]*	This paper	UR945
C. elegans strain: *him-5(e1490) V; fsEx457 [Psrbc-64::tra-2(ic)::SL2::mCherry; Pelt-2::GFP line 1]*	This paper	UR948
C. elegans strain: *him-5(e1490) V; fsEx458 [Psrbc-64::tra-2(ic)::SL2::mCherry; Pelt-2::GFP line 2]*	This paper	UR949
C. elegans strain: *him-5(e1490) V; fsEx461 [Psrh-220::tra-2(ic)::SL2::mCherry; Pelt-2::GFP line 1]*	This paper	UR963
C. elegans strain: *him-5(e1490) V; udEx212[Pelt-2::GFP; Psrh-142::GFP; Psrh-142::ced-3(p15); Psrh-142::ced-3(p17) line 2]*	M. Kryzanowski and D. Ferkey; This paper	UR987
C. elegans strain: *him-5(e1490) V; fsIs15[Prab-3::fem-3(+)::outron::mCherry +Punc-122::GFP]; fsEx449[Psrh-142::tra-2(ic)::mcherry unc-54; Pelt-2::gfp line 1]*	This paper	UR999
C. elegans strain: *him-5(e1490) V; fsEx478[Psrh-142::fem-3(+)::SL2::mCherry; Pelt-2::GFP line 1]*	This paper	UR1004
C. elegans strain: *him-5(e1490) V; fsEx482[Pssu-1::tra-2(ic)::SL2::mCherry; Pelt-2::GFP line 1]*	This paper	UR1026
C. elegans strain: *pha-1(e2123) III; him-5(e1490) V; syEx1249[Psrh-142::GCaMP3; pha-1(+)]*	[67]; this paper	UR1031
C. elegans strain: *pha-1(e2123) III; him-5(e1490) V; fsEx478[Psrh-142::fem-3::mCherry::SL2::unc-54; Pelt-2::gfp]; syEx1249[Psrh-142::GCaMP3+pha-1(+)]*	[67]; this paper	UR1034
C. elegans strain: *pha-1(e2123) III; him-5(e1490) V; fsEx449[Psrh-142::tra-2(ic)::mCherry; Pelt-2::gfp]; syEx1249[Psrh-142::GCaMP3; pha-1(+)]*	[67]; this paper	UR1053
C. elegans strain: *unc-13(e51) I; pha-1(e2123) III; him-5(e1490) V; syEx1249[Psrh-142::GCaMP3; pha-1(+)]*	[67]; this paper	UR1111

REAGENT or RESOURCE	SOURCE	IDENTIFIER
C. elegans strain: *unc-13(e51) I; him-5(e1490) V*	*Caenorhabditis* Genetics Center; this paper	UR1112
C. elegans strain: *unc-13(e51) I; daf-22(m130) II; him-5(e1490) V*	*Caenorhabditis* Genetics Center; this paper	UR1113
C. elegans strain: *srd-1(eh1) II; him-5(e1490) V*	*Caenorhabditis* Genetics Center; this paper	UR1114
C. elegans strain: *tph-1(mg280) II; him-5(e1490) V*	*Caenorhabditis* Genetics Center; this paper	UR1115
C. elegans strain: *him-5(e1490) V; fsEx527[1.5kb MAB-3::GFP (pDZ162) + cc::GFP line 2]*	This paper	UR1131
C. elegans strain: *mab-3(e1240) II; him-5(e1490) V; fsEx547[srh-142p::mab-3::mCherry; Pelt-2::gfp line 1]*	This paper	UR1185
C. elegans strain: *mab-3(e1240) II; him-5(e1490) V; fsEx548[srh-142p::mab-3::mCherry; Pelt-2::gfp line 2]*	This paper	UR1186
C. elegans strain: *mab-3(e1240) II; him-5(e1490) V; fsEx549[srh-142p::mab-3::mCherry; Pelt-2::gfp line 4]*	This paper	UR1187
C. elegans strain: *mab-3(e1240) II; him-5(e1490) V; udEx212[Pelt-2::gfp; Psrh-142::gfp; Psrh-142::ced-3(p15); Psrh-142::ced-3(p17) line 1]*	This paper	UR1188
C. elegans strain: *mab-3(e1240) II; him-5(e1490) V; udEx213[Pelt-2::gfp; Psrh-142::gfp; Psrh-142::ced-3(p15); Psrh-142::ced-3(p17) line 2]*	M. Kryzanowski and D. Ferkey; this paper	UR1189
C. elegans strain: *mab-3(e1240) II; him-5(e1490) V; fsEx479[Psrh-142::fem-3::mCherry; Pelt-2::gfp line 2]*	M. Kryzanowski and D. Ferkey; this paper	UR1190
C. elegans strain: *him-5(e1490) V; fsEx527[1.5kb MAB-3::GFP (pDZ162) + cc::GFP line 2]; fsEx478[Psrh-142::fem-3(+)::SL2::mCherry; Pelt-2::GFP line 1]*	M. Kryzanowski and D. Ferkey; this paper	UR1195
Oligonucleotides		
Psrh-142(ADF)f: CACATGTGACATCTCCGTTAAA	IDT	
Psrh-142(ADF)r: ATTGGCAAAAAGAAAAAAGAGG	IDT	
Psrbc-64(ASK)f: CTGCTGTGAAGTCGACTTCTTCT	IDT	
Psrbc-64(ASK)r: TTTTCAGACTGTGACAAGAAAACTG	IDT	
Psrh-220(ADL)f: GACAGAGCTCATTTCTTTTGG	IDT	
Psrh-220(ADL)r: ACTTGAGTTTGGACCGAAAA	IDT	
Pgpa-4(ASI)f: CTATTTTCGACCATAAAATTCAGA	IDT	
Pgpa-4(ASI)r: TGTTGAAAAGTGTTCACAAAATG	IDT	
Pssu-1(ASJ)f: TCCAGAAAATCTGAAAATCTGAGA	IDT	
Pssu-1(ASJ)r: TCATCGGTGGGGTCCG	IDT	
Recombinant DNA		
Posm-5::tra-2(ic)::SL2::mCherry	This paper	
Prab-3::tra-2(ic)::SL2::mCherry	This paper	
Psrh-142::tra-2(ic)::SL2::mCherry	This paper	
Pgpa-4::tra-2(ic)::SL2::mCherry	This paper	
Psrbc-64::tra-2(ic)::SL2::mCherry	This paper	
Psrh-220::tra-2(ic)::SL2::mCherry	This paper	
Psrh-142::fem-3(+)::SL2::mCherry	This paper	
Pssu-1::tra-2(ic)::SL2::mCherry	This paper	
MAB-3::GFP	[30]	pDZ162

REAGENT or RESOURCE	SOURCE	IDENTIFIER
Software and Algorithms		
AxioVision 4.8	Carl Zeiss	
NeuroTracker	[46, 104]	
ImageJ	[105]	
Pylon viewer	Basler A.G.	
Modified Parallel Worm Tracker	[102]; this paper	
WormExploration Matlab script	This paper	